TOWARDS A BETTER MATHEMATICAL MODELING OF THE GAS-PHASE PROCESSES IN ELECTRON-BEAM FLUE GAS TREATMENT

Valentina GOGULANCEA[1], Vasile LAVRIC[2]

The electron beam technology has been developed successfully for the removal of sulfur and nitrogen oxides from flue gases. The mathematical model presented in the paper aims to provide a better understanding of this innovative process. The kinetics, involving 87 chemical reactions, were assembled from various sources, and integrated into a first principles based mathematical model, consisting of a system of 50 unsteady-state mass balance equations. The results are in satisfactory agreement with published data from industrial and laboratory scale experiments.

Keywords: flue gas treatment, electron beam, plasma chemistry, mathematical modelling, NO_x and SO_2 removal

1. Introduction

Growing environmental concerns have led to stricter regulations regarding the pollutant emissions responsible for climate change, acidification and eutrophication, mainly NO_x, SO_2, VOC's, Hg and CO_2. Despite the considerable decline of the emission levels for both SO_2 and NO_x compared to the year 1991, further reductions are still required and new and better technologies are being developed to reach this goal [1].

The electron beam flue gas treatment (EBFGT) was invented in Japan in the 1970's and was specifically designed for the simultaneous abatement of SO_2 and NO_x. As pilot plants in South Korea, USA, Germany, Japan, China, Poland and Bulgaria have demonstrated, the EBFGT is advantageous from both technological and economical points of view. The first industrial facility for the EBFGT in Europe was built in Poland and has the capacity to treat 270,000 Nm^3/h of flue gases with removal efficiencies of up to 95% for SO_2 and up to 70% for NO_x [2].

The working principle of the EBTFG is the ionization of flue gases due to the interactions of chemical species with fast electrons, involving physico-

[1] PhD student, Chemical and Biochemical Engineering Department, University POLITEHNICA of Bucharest, Romania, e-mail: v.gogulancea@gmail.com

[2] Prof, Chemical and Biochemical Engineering Department, University POLITEHNICA of Bucharest , Romania

chemical processes at different time scales, which have as result a significant decrease in the concentration of toxic impurities. The sulfuric acid formed according to these plasma – chemical reactions and the water vapour present in the flue gas condense together and give rise to a liquid phase, dispersed as liquid droplets. Thus, the irradiation with electron beams takes place in the liquid phase as well, inducing multiple chains of reactions. Consequently, as the mechanism of the EBFGT is extremely complex, developing a mathematical model to accurately describe it has proven to be difficult, even when only the gas phase is considered.

The mathematical models discussed in the literature vary in size and complexity, ranging from only 54 chemical reactions and 28 chemical species [3], to over 900 chemical reactions and almost 200 species [4]. The newly developed mathematical model discussed in this paper starts from a moderately complex kinetics and is improved by adding the necessary reactions aimed to bring its predictions closer to the experiments.

2. Physical model

The electron beam treatment process is based on the conversion of the pollutant species, NO_x and SO_2, into their corresponding acids (HNO_2, HNO_3 and H_2SO_4) by irradiation with accelerated electrons. The acids are converted into salts by addition of neutralizing species (most commonly ammonia) and removed from the flue gas by a dry electrostatic precipitator.

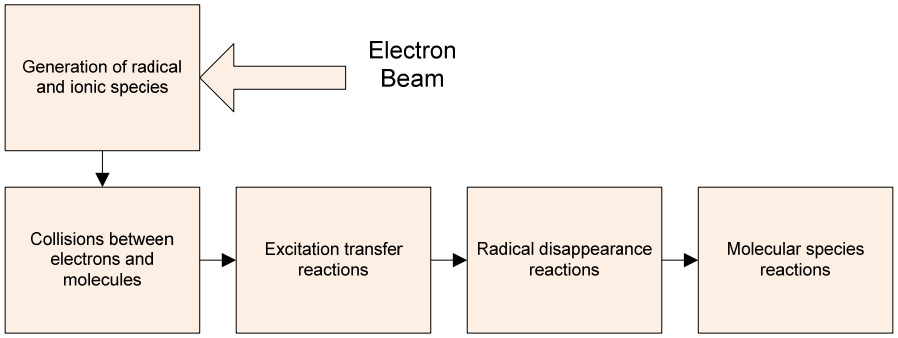

Fig. 1. Main steps of the electron beam treatment mechanism

The sequence of transformations of the initial chemical substances (a typical flue gas contains N_2, O_2, CO_2, H_2O, NO_x, SO_2 and NH_3) and the radiation energy into products qualifies the electron beam treatment as a plasma-chemical process. High energy electrons, generated by the electron gun, interact with the flue gas components rapidly due to their low mass and high mobility. These electrons transmit their energy to the rest of the plasma components, which

undergo ionization, excitation, dissociation, and other plasma – chemical processes as depicted in Fig.1.

Radiation energy is absorbed by the gas components directly proportional to their molar fraction in the mixture. The primary radiolysis phenomena are described by eqs. (1 – 4). The coefficients for each chemical species represent their radiochemical yield - *the number of species transformed by radiation per eV of absorbed energy* – and were taken from [4].

$$4.14\,N_2 \rightarrow 0.885\,N^2D + 0.295\,N^2P + 1.87\,N^4P + 2.27\,N_2^+ + 0.69\,N^+ + 2.96\,e^- \quad (1)$$

$$5.3\,O_2 \rightarrow 2.98\,O + 2.25\,O^1D + 2.07\,O_2^+ + 1.23\,O^+ + 3.3e^- \quad (2)$$

$$6.7\,H_2O \rightarrow 0.51\,H_2 + 4.25\,OH + 4.15\,H + 0.46\,O^3P + 1.99\,H_2O^+ + 1.99e^- \quad (3)$$

$$7.54\,CO_2 \rightarrow 4.72\,CO + 5.16\,O + 2.24\,CO_2^+ + 0.51\,CO^+ + 0.07\,O^+ + 2.82e^- \quad (4)$$

The SO_2 removal is based on two different pathways: the thermal and the radiation – induced processes. In the absence of irradiation, SO_2 removal starts with the thermal reaction of SO_2 and NH_3 to give $(NH_3)_2SO_2$, then continues in the presence of water and oxygen till the final, stable product is obtained, namely $(NH_4)_2SO_4$. The reaction series takes place in the gas phase as well as on the walls of the irradiation chamber and on the surface of the filter.

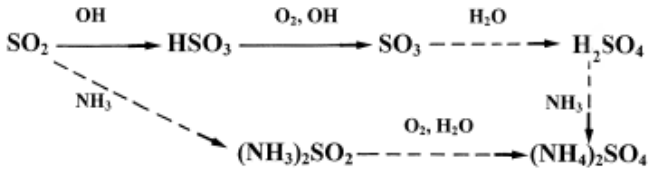

Fig.2. Removal mechanism for sulfur dioxide

Nitrogen oxides are removed only as the result of radiation induced chemical reactions; the main transformations taking place are schematically presented in Fig.3.

3. Mathematical model

The main physico – chemical steps which take place during the EBTFG process include energy absorption of electron beam with active species generation, plasma – chemical reactions in gas phase, aerosol formation and growth, and liquid – phase radiation induced chemical reactions.

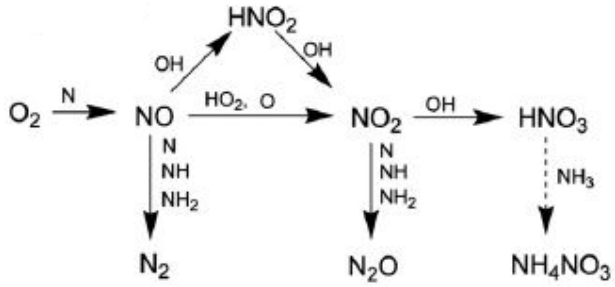

Fig.3. Removal mechanism for nitrogen oxides

The mathematical model discussed in this paper takes into account the first two steps only, in order to simplify the analysis. The latter two will be added in a further work, as the gas phase processes will be satisfactorily described.

The mathematical model is based on two main assumptions: *a)* the energy absorbed by irradiation is evenly distributed and is proportional to the species' concentration in the gas phase and *b)* the flue gas (FG) is taken as ideal and all mass and momentum transfer resistances are neglected.

The original model was assembled using the chemical reactions and their corresponding rate constants given by [5] and listed in ***Table 1***. A mass balance, in the form of a system of ordinary differential equations, was written to describe the behaviour of the chemical species during irradiation with accelerated electrons, using Eq. (5) proposed by [5]:

$$\frac{dc_i}{dt} = G_i \cdot D^* \cdot X_i + rate\ of\ formation - rate\ of\ decomposition \quad (5)$$

where c_i represents the concentration of the reactive species i; D^* is the irradiation rate (kGy/s); X_i denotes the molar fraction of the species i and G_i is the corresponding radiochemical yield, defined as the number of molecules or ions produced or destroyed per 100 eV of absorbed ionizing energy.

The first term on the right-hand side accounts for the generation of reactive species via irradiation while the rates of formation and disappearance are associated to the chemical reactions involving the components of the gas.

Table 1

Chemical Reactions Considered in the Initial Model

No	Chemical reaction	Rate Constants
1	$N_2^+ + NO \rightarrow NO^+ + N_2$	$5*10^{-10}$
2	$N_2^+ + e^- \rightarrow 2N$	$1*10^{-7}$
3	$NO^+ + e^- \rightarrow N + O$	$4*10^{-7}$
4	$NO_+ + e^- \rightarrow NO$	$1*10^{-12}$
5	$NO_2 + e^- \rightarrow NO_2^-$	$8*10^{-28}*[N_2]$
6	$NO^+ + NO_2^- \rightarrow NO + NO_2$	$3*10^{-7}$
7	$N + NO \rightarrow N_2 + O$	$2.2*10^{-11}$
8	$N + NO_2 \rightarrow 2NO$	$25.9*10^{-12}$

9	$N + NO_2 \rightarrow N_2O + O$	$7.7*10^{-12}$
10	$N + NO_2 \rightarrow N_2 + O_2$	$1.8*10^{-12}$
11	$N + NO_2 \rightarrow N_2 + 2O$	$2.3*10^{-12}$
12	$N + N_2O \rightarrow NO + N_2$	$1*10^{-12}$
13	$N + N \rightarrow N_2$	$3.8*10^{-33}*[N_2]$
14	$O + NO \rightarrow NO_2$	$5.4*10^{-32}*[N_2]$
15	$O + NO_2 \rightarrow NO + O_2$	$7.7*10^{-12}$
16	$O + O \rightarrow O_2$	$1.6*10^{-33}*[N_2]$
17	$N4S + NO \rightarrow N_2 + O3P$	$2.2\cdot *10^{-11}$
18	$N4S + NO_2 \rightarrow 2NO$	$5.9\cdot *10^{-12}$
19	$N4S + NO_2 \rightarrow N_2O + O$	$7.7*10^{-12}$
20	$N4S + NO_2 \rightarrow N_2 + O_2$	$1.8*10^{-12}$
21	$N4S + NO_2 \rightarrow N_2 + 2O$	$2.3*10^{-12}$
22	$N4S + O_2 \rightarrow NO + O$	$1*10^{-16}$
23	$N4S + O_3 \rightarrow NO + O_2$	$3.7*10^{-13}$
24	$N4S + N4S + N_2 \rightarrow 2N_2$	$5*10^{-33}$
25	$N2D + N_2O \rightarrow NO + N_2$	$1.6*10^{-12}$
26	$N2D + NO \rightarrow N4S + NO$	$5.9*10^{-11}$
27	$N2D + O_2 \rightarrow NO + O$	$5.2*10^{-12}$
28	$O + NO \rightarrow NO_2$	$3.9*10^{-33}\exp(975/T)*[N_2]$
29	$O + NO_2 \rightarrow NO + O_2$	$3.2*10^{-11}\exp(-535/T)$
30	$O + NO_2 \rightarrow NO_3$	$1.5*10^{-31}*[N2]$
31	$O + O_2 \rightarrow O_3$	$1.1*10^{-34}\exp(510/T)*[N_2]$
32	$O + O_3 \rightarrow 2O_2$	$1.5*10^{-11}\exp(-2240/T)$
33	$O + O \rightarrow O_2$	$1.6*10^{-33}*[N_2]$
34	$NO + O_3 \rightarrow NO_2 + N_2$	$9.5*10^{-13}\exp(-1300/T)$
35	$NO + NO_3 \rightarrow 2NO_2$	$8.7*10^{-12}$
36	$NO_2 + NO_3 \rightarrow NO + NO_2 + O_2$	$4*10^{-16}$
37	$NO_2 + NO_3 \rightarrow N_2O_5$	$6.5*10^{-32}*[N_2]$
38	$N_2O_5 \rightarrow NO_2 + NO_3$	$5*10^{-21}*[N_2]$
39	$CO_2^+ + O_2 \rightarrow O_2^+ + CO_2$	$6.5*10^{-9}T^{-0.78}$
40	$CO_2^+ + H_2O \rightarrow H_2O^+ + CO_2$	$1.7*10^{-9}$
41	$O^+ + CO_2 \rightarrow O_2^+ + CO$	$1*10^{-9}$
42	$CO^+ + O_2 \rightarrow O_2^+ + CO$	$1*10^{-10}$
43	$CO^+ + H_2O \rightarrow H_2O^+ + CO$	$1.3*10^{-10}$
44	$CO^+ + CO_2 \rightarrow CO_2^+ + CO$	$8.5*10^{-10}$
45	$CO_2^+ + O_2^- \rightarrow CO_2 + O_2$	$4*10^{-7}(300/T)^{0.5}+3*10^{-25}(300/T)^{2.5}*[M]$
46	$CO_2^+ + e \rightarrow CO + O$	$4*10^{-7}(300/T)^{0.5}$
47	$CO_2^+ + e \rightarrow CO_2$	$6*10^{-27}(300/T)^{0.5}*[M]$
48	$CO^+ + O_2^- \rightarrow CO_2 + O$	$4*10^{-7}(300/T)^{0.5} + 3*10^{-25}(300/T)^{2.5}*[M]$
49	$CO^+ + e^- \rightarrow CO$	$6*10^{-27}(300/T)\text{^}^{2.5}*[M]$
50	$N_2^+ + CO_2 \rightarrow N_2 + CO_2^+$	$8.3*10^{-10}$
51	$N^+ + CO2 \rightarrow N + CO_2^+$	$1.3*10^{-9}$
52	$CO + OH \rightarrow CO_2 + H$	$1.5*10^{-13}$
53	$N + CO_2 \rightarrow NO + CO$	$4*10^{-13}$
54	$NO_3 + CO \rightarrow NO_2 + CO_2$	$1.6*10^{-11}\exp(-3250/T)$
55	$SO_2 + OH \rightarrow HSO_3$	$5E^{-31}(300/T)^{3.3}*[M]$

56	$SO_2 + HO_2 \rightarrow SO_3 + OH$	$1.49E^{-15}$
57	$SO_2 + O \rightarrow SO_3$	$6.64*10^{-14}$
58	$SO_3 + H_2O \rightarrow H_2SO_4$	$9.91*10^{-13}$
59	$HSO_3 + OH \rightarrow H_2SO_4$	$8.3*10^{-12}$
60	$HSO_3 + OH \rightarrow SO_3 + H_2O$	$8.3*10^{-12}$
61	$HSO_3 + NO_2 \rightarrow HOSO_2ONO$	$8.3*10^{-13}$
62	$HSO_3 + O_2 \rightarrow HOSO_2O_2$	$6.64*10^{-14}$
63	$HSO_3 + HO_2 \rightarrow H_2SO_5$	$8.3*10^{-12}$
64	$HSO_3 + HSO_3 \rightarrow H_2S_2O_6$	$5*10^{-13}$
65	$HOSO_2O_2 + NO \rightarrow HSO_4 + NO_2$	$8.3*10^{-12}$
66	$HOSO_2O_2 + NO \rightarrow HOSO_2ONO_2$	$8.3*10^{-14}$
67	$HOSO_2O_2 + SO_2 \rightarrow HSO_4 + SO_3$	$1.66*10^{-12}$
68	$HSO_4 + NO \rightarrow HOSO_2ONO$	$1.66*10^{-12}$
69	$HOSO_2O_2 + N \rightarrow HSO_4 + NO$	$5.81*10^{-12}$
70	$SO_3 + O \rightarrow SO_2 + O_2$	$7*10^{-13}$

The mathematical model was coded using Matlab® programming environment and was solved using a 2-3 order semi-implicit method for stiff differential equations in house written.

4. Results and Discussions

The first set of simulations was conducted using the kinetic system presented in Table 1. The predictions of the model reproduced well the experimental conditions presented in [6].

As the dose of irradiation is one of the most important parameters for the EBFGT, simulations were conducted with doses ranging from 10 kGy up to 50 kGy. The composition of the flue gas (see Table 2) was also varied to observe the effect of the pollutant's concentration on the removal efficiency.

Table 2

Chemical composition of the flue gas

Species	Concentration (%v)
O_2	7.5
H_2O	14
CO_2	8
N_2	up to 100%

Fig. 4 depicts the variation of the removal efficiency for nitrogen oxide at different initial concentrations: 100, 150, 200, 250, 350 and 500 ppm while maintaining the initial concentration of sulfur dioxide at 500 ppm. The effect of the irradiation dose is higher for the lower initial concentration of NO (see Fig. 4, the slope of the curves, decreasing as the initial concentration of NO increases), reaching almost 100% for doses of 40 and 50 kGy. In the case of higher initial

concentrations, the removal efficiency diminishes accordingly, from around 80% to 42%, for doses as high as 50 kGy.

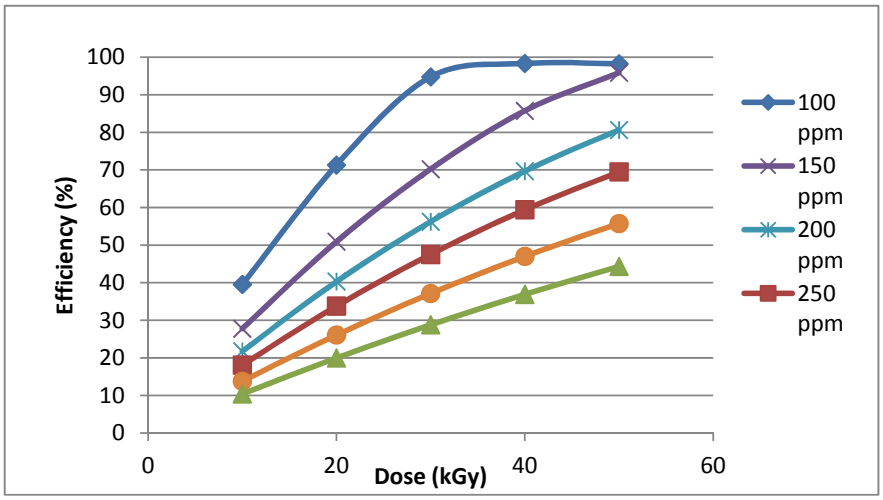

Fig. 4. NO removal efficiency vs. dose

The results obtained are in good agreement with the experimental values presented in [6] and the simulation results in [5] but are still relatively far from the efficiencies reported in industrial installations.

The dependence of the efficiency on the initial concentration of pollutants is even more obvious in the case of the sulfur dioxide, presented in Fig. 5. The initial concentration of SO_2 was varied similarly to the one of nitrous oxide, while the latter's initial concentration was kept at 250 ppm during this new runs. The removal efficiency for sulfur dioxide varies from 17 to 100% function of the initial concentration of the pollutant. Once again, the efficiency is higher for smaller pollutant concentrations. At relatively small concentrations of sulfur dioxide, the removal efficiency shows an exponential increase with the irradiation dose, while at higher concentration, the dependency is almost linear. However, the irradiation dose has a smaller effect on the removal efficiency than reported in literature [7].

The removal efficiencies for nitrogen oxides obtained from the computer simulations are consistent with the ones reported in the experimental work presented in [6]. Nevertheless, they are not in good agreement with the data reported from industrial experience.

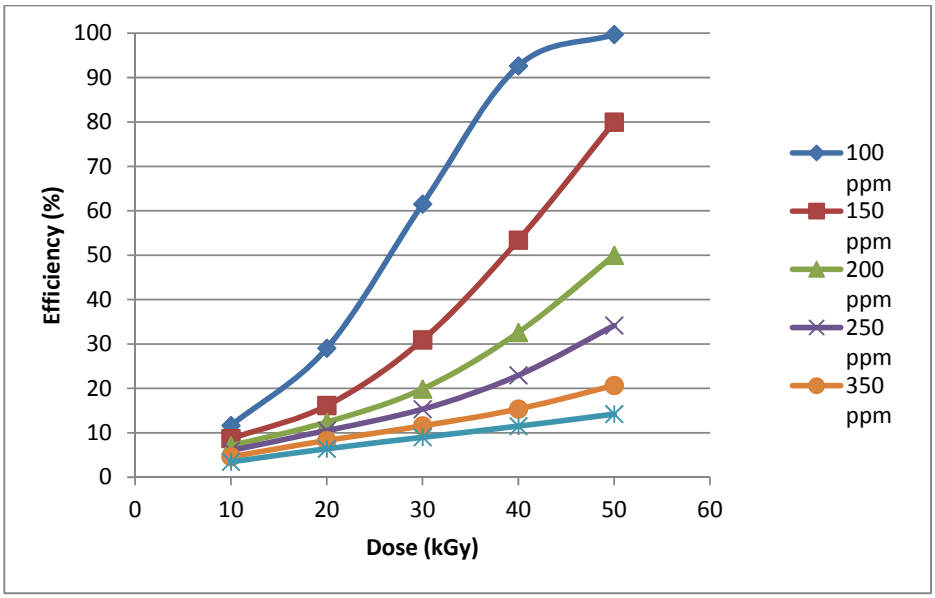

Fig. 5. SO_2 removal efficiency vs. Dose

This fact is explained by the absence of ammonia from the irradiation chamber. Ammonia is added to convert the sulfuric and nitric acids to the corresponding ammonia salts, which are valuable by-products of the process and can be sold as fertilizers. The ammonia is added stoichiometrically with respect to the amount of sulfur and nitrogen oxides in the flue gas as it was shown experimentally that this ratio leads to the highest overall removal efficiency [8].

To account for the presence of ammonia and to quantify its effects on the removal of SO_2 and NO_x, a set of 16 new reactions was selected from literature and added to the existing model. The reactions along with their kinetic constants and source are listed in Table 3**Error! Reference source not found.**.

The reactions (83) and (84) were employed to model the thermal removal of sulfur dioxide, which increases the overall removal efficiency. Even though the thermal mechanism of removing SO_2 is more complex and includes several reactions, the overall efficiency of the process can be expressed only as a function of the initial ammonia and sulfur dioxide concentration, to the best of authors knowledge [9].

Table 3

Additional chemical reactions involving ammonia

No	Chemical reaction	Rate constant	Reference
71	$NO + NH \rightarrow N_2 + OH$	4.75 *10-11	[3]
72	$NO + NH_2 \rightarrow N_2 + H_2O$	2.15 *10-11	[3]

73	$NO + OH + N_2 \rightarrow HNO_2 + N_2$	$7.45*10\text{-}31\ (T/300)^{-2.4}$	[3]
74	$NO_2 + OH + N_2 \rightarrow HNO_3 + N_2$	$2.65*10\text{-}30\ (T/300)^{-2.7}$	[3]
75	$NO_2 + HO_2 + N_2 \rightarrow HNO_3 + N_2 + O$	$1.85*10\text{-}31\ (T/300)^{-3.2}$	[3]
76	$NH_3 + e^- \rightarrow NH + H_2 + e^-$	$9.35 \cdot 10^{-11}$	[3]
77	$NH_3 + e^- \rightarrow NH_2 + H + e^-$	$3.25 \cdot 10^{-10}$	[3]
78	$HNO_2 + NH_3 \rightarrow NH_4NO_2$	$1.05 \cdot 10^{-8}$	[3]
79	$HNO_3 + NH_3 \rightarrow NH_4NO_3$	$1.05 \cdot 10^{-8}$	[3]
80	$NH_3 + OH \rightarrow H_2O + NH_2$	$3.25*10^{-12}EXP(-925/T)$	[3]
81	$OH + O_3 \rightarrow HO_2 + O_2$	$1.35*10^{-12}EXP(-956/T)$	[3]
82	$H_2SO_4+NH_3 \rightarrow NH_4HSO_4$	$1.89*10^{-16}$	[10]
83	$NH_4HSO_4+NH_3 \rightarrow (NH_4)_2SO_4$	$6.6423*10^{-15}$	[10]
84	$SO_2 + 2NH_3 \rightarrow (NH_4)_2SO_4$	$1.52*10^{-30}\ exp(9000/T)$	[9]
85	$SO_2 + 2NH_3 \rightarrow (NH_4)_2SO_3$	$1.01*10^{-31}\ exp(9000/T)$	[9]
86	$O + OH \rightarrow HO_2$	$9.2*10^{-6}$	[4]

The results given by the improved mathematical model for the removal of NO show significantly higher efficiencies at lower irradiation doses – as presented in Fig.6. The results obtained by this mathematical model are in satisfactory agreement with other theoretical and empirical models presented in literature, as opposed to the first model presented.

In the case of sulfur dioxide (see Fig.7), adding ammonia reversed the effect of initial concentration of the pollutant upon the removal efficiency; higher removal efficiencies were obtained for higher initial concentrations. This result can be explained by the contribution of the thermally induced removal mechanism – which at higher inlet concentrations has a larger overall rate. However, the removal efficiency is scarcely affected by the variation of the irradiation dose and the computed removal efficiency is much lower than the ones reported experimentally [2, 7].

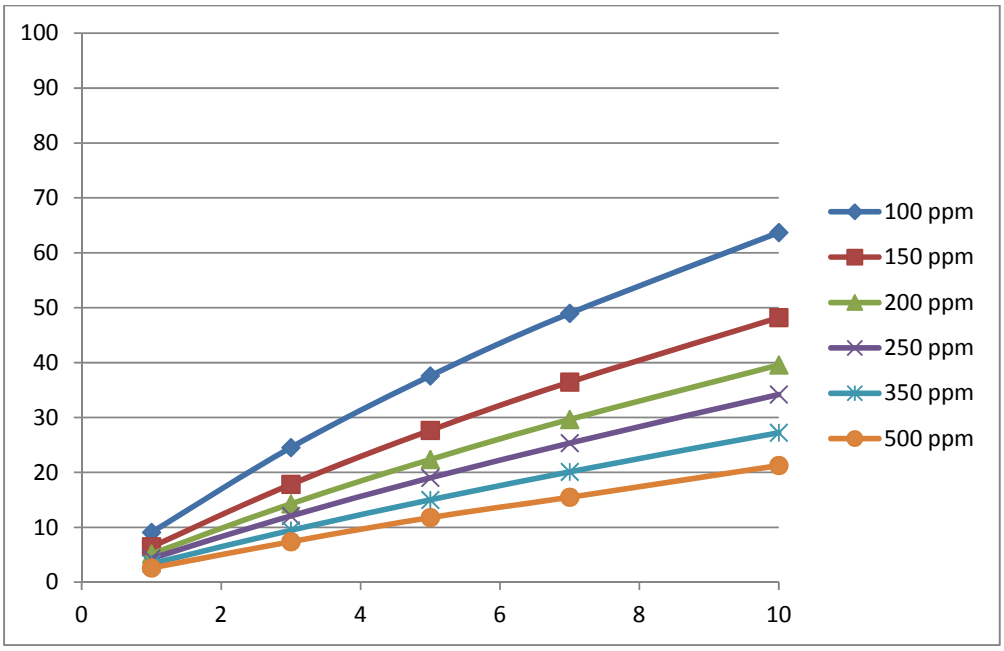

Fig. 6. NO removal efficiency vs. dose

The poor removal of sulfur dioxide can be explained by the exclusion from the mathematical model of the physico – chemical phenomena taking place in the liquid phase during the EBFGT. Another reason for the reduced removal efficiency is the elevated temperature of the process (100°C); as observed from their activation energy, the thermal reactions adversely influenced by the raise of the temperature. Analyzing the removal efficiency of SO_2 at zero irradiation and comparing it to the results presented in Fig. 7, we concluded that the thermal mechanism accounts for approximately 90% of the overall removal of SO_2.

5. Conclusions

The modelling work presented in this paper aims to evaluate two of the different chemical kinetic systems, one proposed in the literature and one assembled by the authors, describing the electron beam treatment of flue gases for the simultaneous removal of sulfur and nitrogen oxides.

The results obtained from the first mathematical model showed a poor agreement with the experimental data for the removal efficiency of the EBFGT presented in literature. This lead to the authors' developing an improved mathematical model by careful selecting and including several other chemical reactions to better explain the electron beam treatment phenomena.

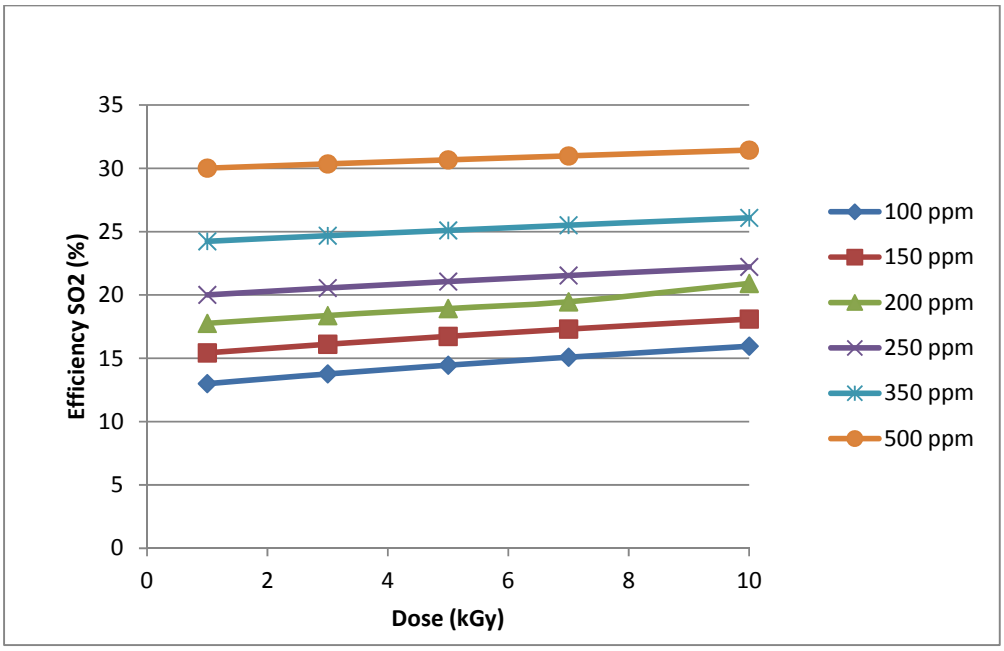

Fig. 7. SO_2 removal efficiency vs. dose

While the behaviour of nitrogen oxide can be predicted with consistency by the second mathematical proposed the removal efficiency of sulfur dioxide is largely underestimated by this model.

The results obtained from the two models tested indicate that further efforts are necessary for developing an accurate mathematical model that can predict the behaviour of a flue gas treatment facility based on electron beam irradiation.

Further modelling work will be focused on determining the actual rates for the chemical reactions of the radiation induced mechanism for the removal of sulfur dioxide and on the inclusion of the liquid phase phenomena.

Acknowledgment

This work is supported by the Sectoral Operational Programme Human Resources Development (SOP HRD), financed from the European Social Fund and the Romanian Government under the contract number POSDRU/159/1.5/S/137390.

REFERENCES

1. *Barbu, A.D.*, Energy and environment report 2008, R. Fernandez, Editor. 2008, EEA.
2. *Chmielewski, A.G., et al.*, Operational experience of the industrial plant for electron beam flue gas treatment. Radiation Physics and Chemistry, 2004. **71**(1-2): p. 441-444.
3. *Dong-Joo Kim, Y.C., and Kyo-Seon Kim*, Effects of Process Variables on NOx Conversion by Pulsed Corona Discharge Process. Plasma Chemistry and Plasma Processing, 2001. **21**(4): p. 625 - 650.
4. *Schmitt, K.L., D.M. Murray, and T.S. Dibble*, Towards a Consistent Chemical Kinetic Model of Electron Beam Irradiation of Humid Air. Plasma Chemistry and Plasma Processing, 2009. **29**(5): p. 347-362.
5. *Zhang, J., et al.*, A scheme for solving strongly coupled chemical reaction equations appearing in the removal of SO2 and NOx from flue gases. Vacuum, 2009. **83**(1): p. 133-137.
6. *Nishimura, K. and N. Suzuki*, Radiation Treatment of Exhaust Gases, (XIV). Analysis of NO Oxidation and Decomposition in Dry and Moist $NO-O_2-N_2$ Mixtures by Computer Simulation. Journal of NUCLEAR SCIENCE and TECHNOLOGY, 1981. **18**(11): p. 878-886.
7. *Basfar, A.A.*, Electron beam flue gas treatment (EBFGT) technology for simultaneous removal of SO2 and NOx from combustion of liquid fuels. Fuel, 2008. **87**(2008): p. 1446–1452.
8. *Chmielewski, A.*, Industrial applications of electron beam flue gas treatment—From laboratory to the practice. Radiation Physics and Chemistry, 2007. **76**(8-9): p. 1480-1484.
9. *Gerasimov, G.Y., et al.*, Homogeneous and heterogeneous radiation induced NO and SO2 removal from power plants flue gases - Modeling study. Radiation Physics and Chemistry, 1996. **48**(6): p. 763-769.
10. *Baek, B.H., V.P. Aneja, and Q. Tong*, Chemical coupling between ammonia, acid gases, and fine particles. Environmental Pollution, 2004. **129**(1): p. 89-98.